Journal of Building Engineering 120 (2026) 115330

Contents lists available at ScienceDirect

Journal of Building Engineering

journal homepage: www.elsevier.com/locate/jobe

Understanding of municipal solid waste incineration (MSWI) bottom ash/cement blends: Impact of natural fiber on mechanical strength and leaching behavior

Helong Song [a,b,c], Florent Gauvin [d], Tao Liu [e,*], Xiaohui Sun [a,b,c,**], Zijun Dong [a,b,c], Feng Wang [a,b,c], Xiangsheng Chen [a,b,c], H.J.H. Brouwers [d]

[a] Key Laboratory of Coastal Urban Soil-Water Environmental Evolution, Ministry of Ecology and Environment (under construction), Shenzhen University, Shenzhen, 518060, China
[b] State Key Laboratory of Intelligent Geotechnics and Tunnelling, Shenzhen University, Shenzhen, 518060, China
[c] College of Civil and Transportation Engineering, the Underground Polis Academy, Shenzhen University, Shenzhen, 518060, China
[d] Department of the Built Environment, Eindhoven University of Technology, P. O. Box 513, MB Eindhoven, 5600, the Netherlands
[e] Construction Materials and Durability, Department of Environmental and Resource Engineering, Technical University of Denmark, Brovej 118, 2800, Kongens Lyngby, Denmark

ARTICLE INFO

Keywords:
Bottom ash
Natural fibers
Binders
Pores
Compressive strength
Leaching behavior

ABSTRACT

There are well-known drawbacks to using municipal solid waste incineration bottom ash (BA) as cement substitution materials: low compressive strength and the leaching of contaminant ions from BA. These drawbacks hinder the practical application of MSWI BA in construction. Conventional strategies, such as steel or synthetic fiber reinforcement and BA washing pre-treatment, can improve performance but often involve increased costs, high water consumption, and the risk of secondary pollution. In this context, natural fibers present a more sustainable alternative due to their high stiffness, renewability, and low embodied energy. This work evaluates the effect of natural fiber incorporation to solve the above issues. Effects of natural fiber types (sisal fibers, SF, and oil palm fibers, OPF) and BA replacement levels (15 wt% and 30 wt%) on compressive strength and porosity were evaluated. Hazardous ions leaching changes were examined using inductively coupled plasma atomic emission spectrometry (ICP–AES) and Ion chromatography (IC). It was observed that when the maximum replacement with BA increased to 30 %, the 28-d compressive strength of the blended binder with SF is about 85 % higher than the reference binder. Leaching tests show that most contaminant ions were effectively mitigated under the experimental conditions. In addition, compared with a pure cement binder, BA-based cement binders with natural fibers have lower greenhouse gas (GHG) emissions and production costs. This study provides a promising solution to effectively apply MSWI BA into the cement binders for potential building materials.

* Corresponding author.
** Corresponding author.
E-mail addresses: taliu@dtu.dk (T. Liu), sunxiaohui@szu.edu.cn (X. Sun).

https://doi.org/10.1016/j.jobe.2026.115330
Received 29 November 2025; Received in revised form 31 December 2025; Accepted 16 January 2026
Available online 21 January 2026

1. Introduction

Global municipal solid waste (MSW) generation is estimated to increase by approximately 1.3 billion tonnes annually, with total generation expected to reach approximately 3.4 billion tonnes by 2050 [1,2]. An enormous amount of MSW is currently deposited through landfilling or incineration [3]. Landfilling is increasingly constrained due to higher fees, largely occupied lands, policy restrictions, and environmental pollutants. In contrast, MSW incineration not only reduces waste mass (by 70 %) and volume (90 %), but also enables energy recovery [4]. Therefore, incineration has become a more widely accepted and effective way to treat solid waste. However, it generates a significant quantity of bottom ash (BA), which accounts for around 80 % by weight of all solid residues produced after incineration [5].

Previous studies [6,7] have shown that BA possesses chemical compositions and pozzolanic activity similar to other supplementary cementitious materials, such as fly ash and silica fume, and ground-granulated blast-furnace slag. These findings indicate that BA can be directly used as a cementitious material to partially replace cement [8]. Nevertheless, its practical application in the construction sector has been hindered by two major issues: (i) leaching of contaminants and (ii) low compressive strength. For instance, the low strength has been attributed to the presence of metallic aluminium in BA [9]. When BA is mixed into a cementitious matrix, metallic aluminium reacts in the alkaline environment and generates hydrogen gas, resulting in pore formation and strength deterioration. To solve this, several treatment strategies have been proposed: (1) physically removing the aluminium from the stony fraction [10]; (2) mechanically milling and sieving out the aluminium fraction [11]; (3) oxidizing the metallic aluminium before utilization [12,13]. For example, Joseph et al. [14] reported that the oxidation reaction of metallic aluminium of milled BA could be accelerated by increasing the water temperature. Although these treatment approaches can effectively reduce the content of metallic aluminium in BA, they also bring some new disadvantages: a complex treatment process and high cost. More importantly, the other core challenge is the leaching of contaminants from BA. BA after the complex MSW incineration contains enormous heavy metals (e.g., Pb, Cu, and Zn) and anions (e.g., soluble chloride and sulphates), which pose a risk to the environment and human health [11,15,16]. Thus, the concentrations of heavy metal ions and anions need to be decreased to meet the requirements of local legislation before the BA can be safely used as a building material. To achieve this, a series of treatment methods, such as water washing repeatedly [17], weathering [18], acid washing [19], and alkaline washing [20], have been adopted. However, these approaches often involve substantial water consumption, high chemical costs, complex processing procedures, and stringent equipment requirements, thereby limiting their economic and environmental feasibility for large-scale implementation. Hence, a simple and cost-efficient approach is urgent to achieve both the strength enhancement and environmental compliance.

In this context, some studies have explored the incorporation of fibers as a relatively simple strategy to improve the performance of BA based-cementitious composites. Various types of fibers, including steel fibers [21], basalt fibers [22], polyvinyl alcohol fibers [23], polypropylene fibers [24], polyethylene fibers [25], and glass fibers [26], have been incorporated to enhance mechanical strength and crack resistance. However, these investigations have largely focused on mechanical performance, with limited consideration of environmental aspects. A few studies have reported that fiber addition may indirectly influence contaminant leaching by modifying the microstructure of cementitious matrices. For example, Youssari et al. [27] observed that metal fiber incorporation densified the cementitious matrix, leading to reduced leaching behavior. Similarly, Zhang et al. [28] discovered that concrete with basalt fibers added can suppress the leaching by increasing the density of the concrete. Nevertheless, the potential role of fibers in influencing contaminant leaching behavior of BA based-cementitious composites has not been investigated. Moreover, the aforementioned fibers are often associated with high embodied energy, increased carbon emissions, and higher material costs, which limit their sustainability and practical applicability. Thus, an alternative, eco-efficient fiber reinforcement materials is needed that can immobilize leaching behavior.

Natural fibers, derived from biomass, exhibit high stiffness, good mechanical strength, sustainability, and low cost [29]. Moreover, they have been widely employed as bio-based sorbents for the removal of heavy metal ions from wastewater [30,31]. Two main mechanisms have been proposed to explain their adsorption behaviour: (1) physical adsorption driven by the unique hollow lumen structure, and (2) ion exchange, whereby positively charged metal ions are attracted to negatively charged functional groups on the fiber surface through electrostatic interactions [32]. In this study, therefore, it is proposed that natural fibers have the potential to absorb the leachate when BA is applied to partially replace cement. Furthermore, it is reported that natural fibers have the advantage of filling the pores caused by the swelling of coal bottom ash [22] or wood bottom ash [33]. In addition, natural fiber incorporation brings other benefits, such as sustainability and low cost. Considering the above factors, natural fiber incorporation appears to be the most feasible solution for solving the above bottleneck problems when BA partially replaces the cement. However, despite this potential, the combined effects of natural fiber incorporation on both strength development and contaminant leaching in BA-based cementitious binders have not yet been systematically explored.

Hence, this study aims to investigate whether the incorporation strategy of natural fibers can simultaneously mitigate both the low mechanical strength and contaminant leaching issues of BA-based cementitious binders (BA-BCBs). Specifically, the study is designed to answer the following research questions.

(i) To what extent can natural fiber incorporation improve the strength performance and pore structure of BA-BCBs?
(ii) How does the presence of natural fibers influence the leaching behavior of contaminant ions of BA-BCBs?
(iii) What are the environmental and economic implications of incorporating natural fibers into BA-BCBs?

Sisal fibers (SF) and oil palm fibers (OPF) were selected as the research objects, as preliminary experiments indicated that these two fibers exhibited superior leachate absorption capacity compared to other commonly used natural fibers (e.g., bamboo fibers, hemp

fibers, coconut fibers, and wood wool fibers). According to the statistics of the Food and Agriculture Organization of the United Nations [34], the annual global production is around 300000 tons for SF and 1940 million tons for OPF, indicating their abundant availability and potential as sustainable materials. In this study, BA was used to replace cement at levels of 15 % and 30 % by weight of the binder. The compressive strength and macro-micro pore distribution of the BA-based cement binders (different replacement rates and different natural fibers) were investigated and analyzed. The microscopic characteristics of the blended binders were further examined using isothermal calorimetry, XRD, and TGA. Additionally, the leaching behavior of heavy metal ions and anions was investigated through ICP-AES and IC. Finally, the environmental impact of proposed binders was assessed using life cycle assessment (LCA) with greenhouse gas (GHG) emissions as the primary indicator, and an economic evaluation was conducted to estimate the associated costs.

2. Materials and methods

2.1. Materials and selected reasons

In this research, the raw materials used to prepare the cement-based binders were the OPC (CEM 52.5 R, ENCI, the Netherlands), MSWI bottom ash (Heros, the Netherlands), and a small number of natural fibers (Wageningen University). The reasons for the addition of natural fibers are that one is to mitigate the leaching of heavy metal ions from the MSWI bottom ash, and the other is to improve the mechanical strength of the cement-based binders.

Before mixing, MSWI BA material was dried and milled for 5 min to meet the PSD requirement as a cementitious supplementary material, as is shown in Fig. 1. The chemical composition of the CEM I 52.5 R and milled BA, determined by using the XRF, is given in Table 1. The summation of the oxides ($SiO_2 + Al_2O_3 + Fe_2O_3$) sample was found to be 69.3 %, close to 70 %; the sulfur content, SO_3, was 1.24 % less than 4 %, and LOI was 8.14 % less than 10 %. So, according to ASTM C618, this type of MSWI bottom ash almost meets all the requirements to be used as a cementitious material. Regarding the natural fiber selection, sisal fibers and oil palm fibers were selected in this study, considering the fiber microstructure (Fig. 2). Besides, the chemical composition of these fibers is further analyzed (Table 2).

2.2. Sample preparation

The composition of the BA-based cement binders (BA-BCBs) is shown in Table 3. Several BA-BCBs mixed with natural fibers were designed to solve the bottleneck problems (leaching & low strength) caused when BA was directly used as the replacement for cement. Therefore, two kinds of 'reference' binders, only mixed BA with cement, are considered and denoted as Ref-15 and Ref-30, respectively.

For the case of the blended binders with two different fibers, the design aimed to further compare the impact of the difference in the cellulosic microstructure and chemical components on the leaching problem and strength property of these binders. The blended binders with sisal fibers were denoted as S-15 and S-30, while those binders with oil palm fibers were denoted as O-15 and O-30. Moreover, to increase the highest possible amount of waste BA application, 30 % wt. of the cement was replaced by BA in this study, which is referred to as the number '30'. Similarly, the number '15' means that the cement replacement ratio with BA is 15 %. The selection of the replacement ratio is based on the preliminary experiments. When the replacement level with BA exceeded 30 %, the compressive strength of the specimens became too low to allow reliable mechanical testing. Thus, the 15 % and 30 % substitution levels were selected in a reasonable and stepwise manner. The design of the binders also considered the potential effect of natural fibers on the actual water/cement ratio; hence, the water absorption capacity of the two natural fibers was tested according to ASTM procedure D570-99 (ASTM 1999). The obtained results were that the water absorption of sisal fiber and oil palm fiber was 3.58 % and 2.51 %, respectively. Finally, in view of the poor absorbing-water ability and low amount of fiber addition, the influence of the natural

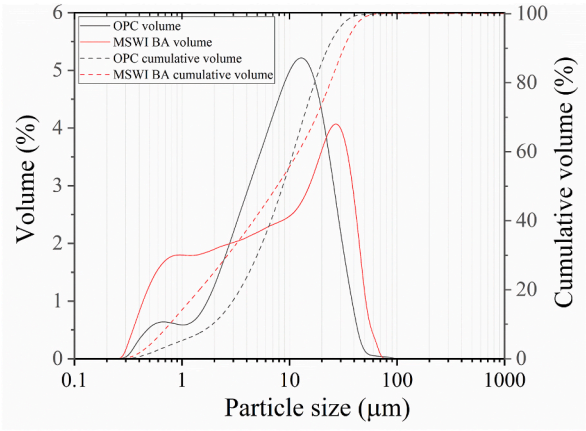

Fig. 1. Particle size distribution of cement and milled BA.

Table 1
Chemical compositions of the CEM 52.5 R and milled BA.

Oxides (%)	Milled BA	Cement 52.5 R
SiO_2	37.9	15.8
CaO	21.9	68.2
Al_2O_3	13.8	6.9
Fe_2O_3	17.7	3.9
K_2O	1.3	0.2
MgO	1.5	1.3
P_2O_5	1.1	–
SO_3	1.3	2.8
CuO	0.7	–
ZnO	0.9	0.1
TiO_2	–	0.4
Other	1.8	0.6
LOI	8.2	1.4
Specific density	2.2 ± 0.1	2.5 ± 0.1

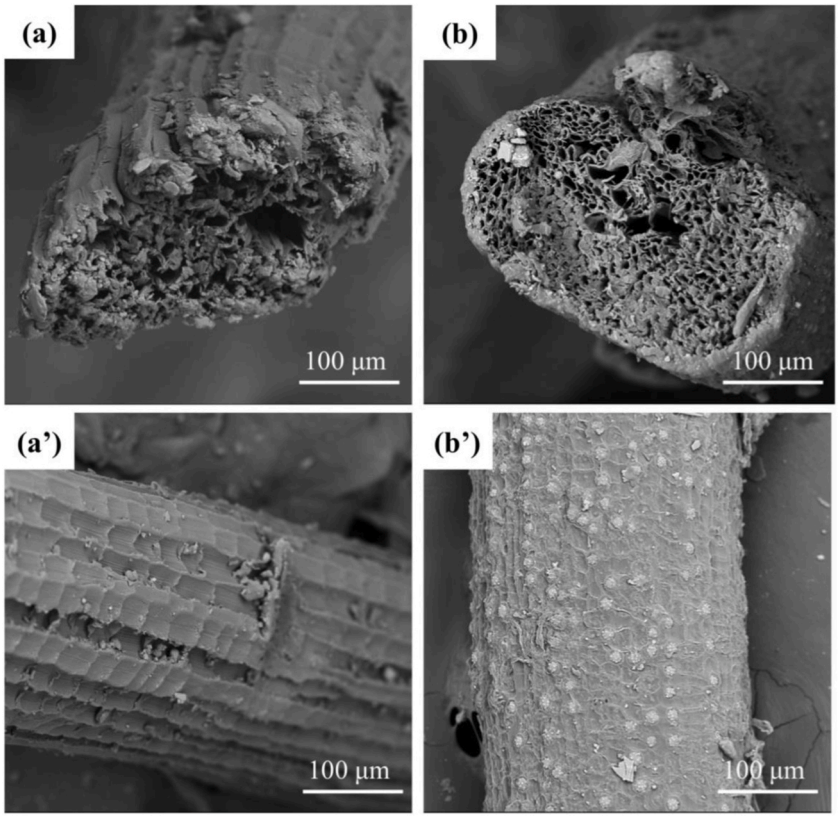

Fig. 2. Microstructure of sisal fiber (a, cross-section; a', surface) and oil palm fiber (b, cross-section: b' surface).

Table 2
Chemical composition of fibers.

Type	Cellulose (%)	Hemicellulose (%)	Lignin (%)	Ash (%)	Extractive (%)	Average diameter (μm)
Sisal fiber [35]	67.0–78.0	10.0–14.2	8.0–11.0	10.0	2.0	150–320
Oil palm fiber [36]	32.8 ± 1.9	42.7 ± 2.0	14.9 ± 0.21	7.8	11.3 ± 0.1	410–650

Noting: the average diameter of sisal fibers and oil palm fibers used in this experiment is statistically calculated.

fiber absorption on the total water/cement ratio in this study could be ignored. However, to keep the similar workability of all specimens and low water usage, the water/cement ratio (0.45) was determined after many preliminary attempts. The CEM 52.5 R was only employed in this work since the effect is faster to achieve the high early-age strength. The fiber incorporation was selected at 2 %.

Table 3
Composition of the BA-BCBs with or without natural fibers.

NO.	Fibers		The proportion of cementitious matrix		
	Oil palm	Sisal	Milled BA	OPC	Water/Binder
Ref-15	–	–	15 %	85 %	0.45
Ref-30	–	–	30 %	70 %	0.45
S-15		2 %	15 %	85 %	0.45
S-30		2 %	30 %	70 %	0.45
O-15	2 %		15 %	85 %	0.45
O-30	2 %		30 %	70 %	0.45

wt of cement, considering optimal enhancement of mechanical properties reported in other literature [37]. At higher fiber contents, achieving uniform fiber dispersion becomes increasingly difficult due to the soft and hydrophilic characteristics of natural fibers, which can negatively affect the homogeneity and performance of the cementitious matrix.

For the specimen preparation, the fibers (SF or OPF) were first mixed with cement and milled BA in a blender (Perrier Labotest, type 32, France) for 90s to ensure homogeneity, followed by the addition of water. After mixing for an additional 2 min, the mixture was cast into plastic molds with dimensions of 40 mm × 40 mm × 160 mm and covered with a damp polyethylene film to minimize water evaporation. The specimens were initially cured at room temperature for 24 h. After demolding, they were sealed again with cling film and cured in a climatic chamber (20 ± 2 °C and 50 ± 5 % RH) until the test ages.

2.3. Characterization

2.3.1. Physical properties

Regarding the raw materials: cement and milled BA, the specific densities were tested by a Helium pycnometer (Accupyc II 1340), and the chemical compositions were measured by X-ray Fluorescence spectrometer (XRF). Loss on ignition (LOI) was evaluated by oven drying 10 g of MSWI BA at 105 °C to constant mass before calcining at 1000 °C for 1 h, cooling, and re-weighing. The particle size distributions (PSD) were measured by laser diffraction (Mastersizer 2000, Malvern). The absorption coefficient of 0.1 was used for both materials; a particle refractive index of 1.68 was used for cement, and 1.54 for milled BA. In terms of natural fibers, their microstructures were characterized by scanning electron microscopy (SEM). The micro-sized pore distribution of the cut specimens (15 × 15 × 10 mm^3) was characterized by Micro-CT 100 (Scanco Medical AG, Switzerland). The detailed parameters for testing are following the literature [38].

2.3.2. Thermogravimetric analysis (TGA)

The thermogravimetric analysis (TGA) and differential thermogravimetry (DTG) study were performed by a Q2000 TA Instrument to illustrate the chemical composition of selected paste samples. The powdered paste samples were heated under nitrogen gas protection from 40 to 800 °C, with a rate of 10 °C/min.

2.3.3. Standard leaching test

The leaching test was conducted in accordance with EN 12457-4, 2002, involving 24 h of agitation at 200 rpm with a liquid/solid ratio of 10. The original BA and six cement paste samples were tested, with the paste samples crushed and sieved to below 4 mm after

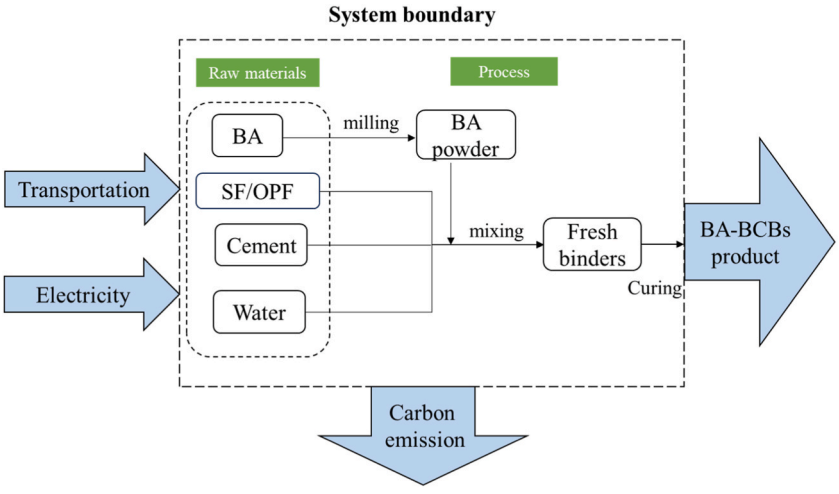

Fig. 3. The system boundary for the BA-BCBs product.

28 days of curing. Following the leaching procedure, the solutions were filtered through 0.2 μm membrane filters for IC and ICP analyses. The filtrates used for ICP–AES analysis were subsequently acidified with 69 % nitric acid (ISO grade). The concentrations of potentially toxic elements (Ba, Cr, Cu, Zn, Mo, Sb), as well as chloride and sulfate ions, were measured in this study. Additionally, Furthermore, we adopted the strict Dutch soil decree [39] to assess the leaching behaviour of paste samples, ensuring compliance with building safety and human health requirements.

2.3.4. Compressive strength

All binder samples of 40 × 40 × 160 mm were submitted to compressive strength testing according to the standard EN 12390–3:2019. All samples were tested after 3 and 28 days of curing. The data is gained by repeatedly testing three times to guarantee reproducibility. The significance of the difference between the experimental samples and reference samples was statistically analyzed by one-way ANOVA, and *P*-value <0.05 was considered statistically significant.

2.4. Life cycle assessment (LCA)

The LCA approach has been used to assess the environmental impact of supplementary cementitious composites [40,41]. The process includes three stages for LCA execution: Goal and scope definition, inventory analysis, impact assessment, and interpretation [42]. In this study, the LCA was conducted using the cradle-to-gate method to evaluate the environmental impact of incorporating natural fibers in the BA-based binders. The system boundary is illustrated in Fig. 3, and the functional unit is considered as one ton of blended binders. This evaluation only focuses on the impact category of greenhouse gas (GHG). LCA modelling was performed using SimaPro software (version 9.0.0.48).

2.4.1. Life cycle inventory (LCI)

In this study, unit processes in the LCI were sourced from the Ecoinvent databases shown in Table 4. The impact assessment was conducted using the ReCiPe midpoint (H) method. The built data of the MSWI bottom ash (including the electricity used in the milling process) was modified based on this experiment. Additionally, the environmental properties of sisal fibers and oil palm fibers were modified based on the system database of jute and kenaf fibers due to their similar agronomic characteristics and processing routes. Nevertheless, such modifications may lead to deviations from actual environmental profiles of SF and OPF. To reduce the associated uncertainty in carbon emission estimates, the carbon footprint values were adjusted according to the carbon content of SF and OPF measured by the elemental analysis. However, other environmental impact categories were not considered in this study, which represents a limitation of the present LCA and should be addressed in future research.

3. Results and discussion

3.1. Compressive performance

3.1.1. Compressive strength

The compressive strength of all binder samples is shown in Fig. 4. The compressive strength of the BA-BCBs is considerably reduced as the amount of replacement with BA increases at both 3 days and 28 days after curing. The fact can be explained by the higher porosity created in the cementitious matrix due to the larger amount of metallic aluminium presented in BA, resulting in the poor strength property of the binders. This finding is consistent with Chen et al. [9] showed that the detrimental effect of metallic aluminium existed in MSWI BA on the compressive strength of concrete due to the release of the hydrogen gas generated by the reaction between metal specimens (e.g., aluminium) and alkali salts. And it is also confirmed by the following analysis of pore distribution. In addition, another potential reason is the lower pozzolanic reaction of BA [43], meaning that large unreacted particles of BA also loosen the compressive strength of the blended binders. Therefore, the reasons for this compressive strength phenomenon are not a single parameter [44] and will specifically be discussed later.

It is clear that the mechanical strength of BA-BCBs increases to some extent with the addition of natural fibers at both replacement levels with BA. This increment is dominantly due to refined pore structure and densified matrix through the fiber filling [45]. Further, it is noted that there is a significant difference ($p < 0.05$) between the sisal fiber samples and the reference samples. This holds irrespective of the level of cement replacement and the duration of curing. The compressive strength for SF incorporation is significantly superior to that of the counterpart reference samples. For samples with the replacement of 30 wt%. BA after 28-d curing, S-30

Table 4
Source of unit process.

Type of Input data	Source
Water	Ecoinvent 3 database, water, the Netherlands
Sisal fibers	Ecoinvent 3 database, jute modified
Oil palm fibers	Ecoinvent 3 database, kenaf modified
Electricity	Ecoinvent 3 database, natural gas, conventional power plant, the Netherlands
MSWI bottom ash	Ecoinvent 3 database, MSWI bottom ash built based on the pre-treated process in this study and the literature
Cement	Ecoinvent 3 database, Cement, Portland
Transportation	Ecoinvent 3 database, lorry 16–32 metric tons, EURO5.

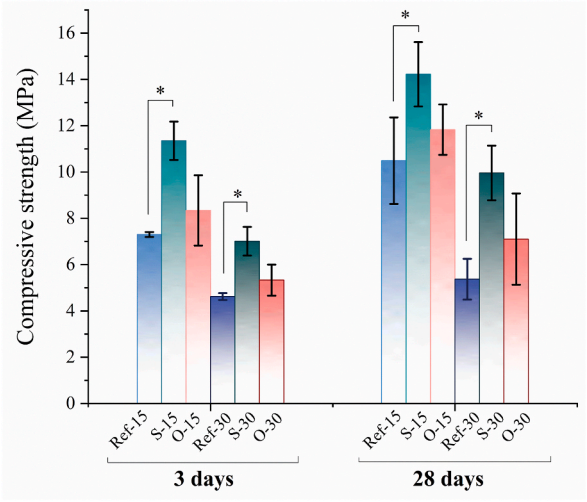

Fig. 4. Compressive strength of the BA-BCBs with different replacement and different natural fibers(the symbol * represents a significant difference).

gains the highest compressive strength (about 10 MPa), up to 85 % increase compared to the Ref-30. On the other hand, no statistically significant difference between the samples with OPF and reference samples was observed, although the OPF incorporation helped in the increment of the BA-BCBs in terms of compressive strength. The difference in strength increment between the two fiber-reinforced BA-BCBs may be associated with the difference in the organic component contents of SF and OPF, which delays the cement hydration reaction. To discuss it further, the cement hydration, setting, and hardening mainly depend on the concentration of lignin and extractives in the natural fiber [46]. Therefore, the binders with sisal fibers, due to the low content of lignin and extractives, have relatively higher compressive strength. From the application of BA for road pavement, the remaining binder groups except Ref-30 and O-30 can meet the compressive strength requirement of road paving in garden parks [47]. Meanwhile, combined with considering the consumption amount of BA, the S-30 is the best candidate.

3.1.2. Pore size distribution

To further evaluate the effect of the physical properties of pores (i.e., numbers, shapes, and size) and factors of the hydration reaction degree on the compressive strength of the binder mixtures, it is important to identify three different phases: pores, reacted, and untreated products in the blended binder samples.

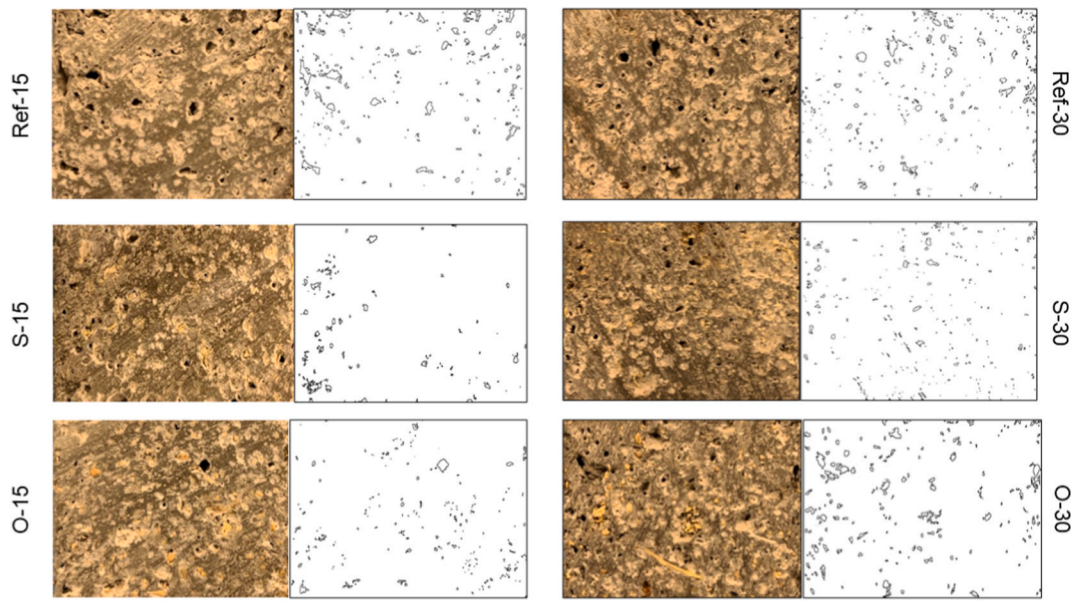

Fig. 5. The distribution of pore areas in different samples using ImageJ software.

The cross-section slices of different samples are processed by using the software ImageJ (Fig. 5). It should be mentioned that the word 'pores' here is regarded as the naked-eye visible pores. The pore structures are visible with dark phases in the physical photos, and with circles shown in schematic pictures. In the physical photos, the light phases represent the unreacted particles (almost unhydrated BA powders due to being less reactive than cement [48]), and the color degree represents the reacted phases between the pores and unreacted particles. For the physical structures of pores, the larger-round pores and irregular-narrow pores are evidently observed, and the pore number is more in Ref-15 and Ref-30. While the other binder samples with natural fibers have relatively few tiny circular pores. Natural fiber incorporation can function as a filler for large pores. For instance, when cement replacement by BA is 15 wt%, S-15 and O-15 are quite denser, with only several fine pores compared to the counterpart's reference, which indicates both SF and OPF play a good role in filling pores. However, when the replacement rate increases to 30 wt%, these two fibers exhibit different filling effects: SF effectively reduces the size and number of pores, but OPF has a relatively poor filling effect with some visible large pores. The most likely reason can be related to the chemical components of natural fibers. As can be seen in Table 2, compared to SF, OPF has more content of lignin and extractives, which significantly delay the cement hydration reaction [49]. Especially, the fewer cement proportions there are, the more pronounced the delaying effect is. It results in a looser skeleton (reacted products) of the BA-based cement binders. Consequently, OPF incorporation could not effectively improve the mechanical strength of the BA-BCB. This view is also consistent with the result of the above-tested compressive strength.

Fig. 6(a) presents a typical greyscale histogram from a 28-day cured binder mixture (O-15). The histogram was transformed into the Gaussian curves using the PeakFit function in the software OriginPro version, in which the Gausses 1, 2, and 3 represent the pores, reacted products, and unreacted products. The threshold values (intersections) between Gauss 1 and Gauss 2 and between Gauss 2 and Gauss 3 were thought to distinguish the pores, reacted products, and unreacted particles, which is shown in Fig. 6(b). With this approach [50], the threshold values and relevant area fractions of all binder samples were listed in Table 5. It can be seen that reference samples without natural fibers have a wider threshold range and a higher pore area fraction than other samples with natural fibers. That means natural fiber incorporation can reduce the porosity of the BA-based cement binders through the filling effect, thus contributing to the improvement of compressive strength. However, the incorporation of natural fibers into the BA-based cement matrix also brings about the retardation of the cement hydration, negatively influencing the strength development. For the S-30 sample, the threshold range representing unreacted particles is wider, and the area fraction of reacted products is lower compared to the Ref-30 sample. From this point of view, the compressive strength of S-30 should be lower than that of the Ref-30 sample. In opposite this expectation, the tested strength results from Fig. 4 show that the compressive strength of S-30 is significantly higher than that of Ref-30. This indicates that the positive effect of SF as a filler role on the compressive strength of the BA-BCBs considerably exceeds the negative effect of it as a "cement retarder". Similar behaviour was visible in the case of OPF incorporation, but the exceeding degree is not evident (Fig. 4), which probably could be explained by the fact that the higher organic components of lignin and extractives (Table 2) enhance its influence as a 'cement retarder'.

In order to further investigate the influence of the natural fibers incorporation on the micro-sized range pores in the BA-based cement binders, Micro-CT is employed to analyze the fine pores (the size of diameter below 2 mm) in all samples after 28-day curing.

The results of micro-size pore distribution and 3-dimensional volume of all binder samples are displayed in Fig. 7. It can be clearly

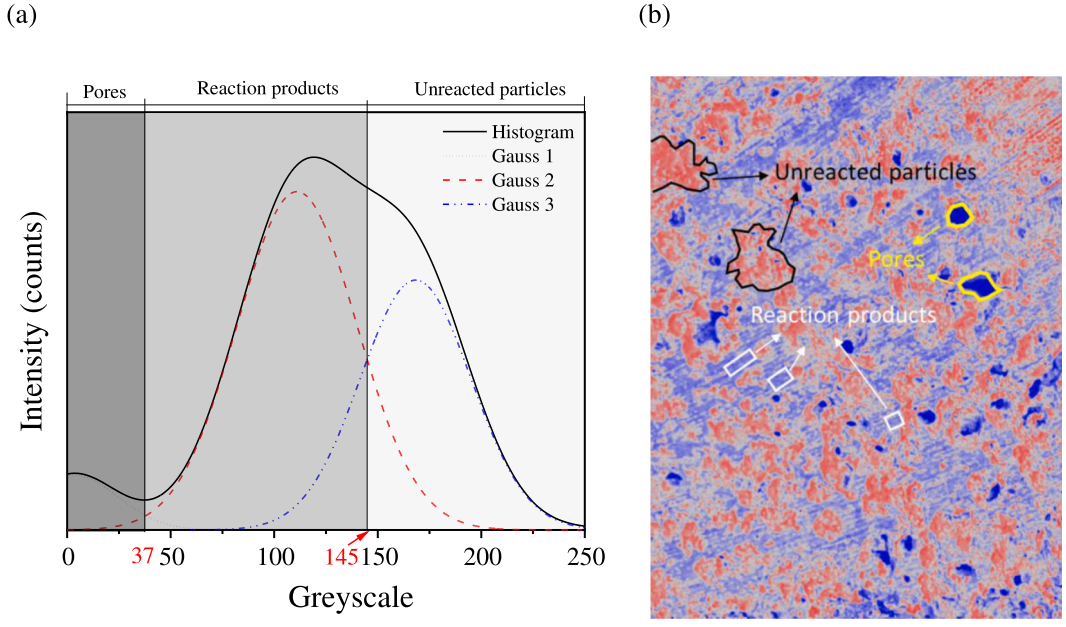

Fig. 6. A typical polychromatic greyscale histogram (a) and a typical cross-section (b) of different phases in the binder samples after 28 days of curing. Noting: Red zones represent unreacted particles; Purple represents reaction products; Blue represents pores.

Table 5
Threshold values and related area fractions for identifying different phases in different samples.

Samples		Pores		Reaction products		Unreacted particles	
		Threshold value range	Area fraction (mm^2/mm^2, %)	Threshold value range	Area fraction (mm^2/mm^2, %)	Threshold value range	Area fraction (mm^2/mm^2, %)
28 days	Ref-15	0–53	10.50 ± 0.08	53–154	55.42 ± 2.03	154–255	32.13 ± 3.08
	S-15	0–43	4.82 ± 0.16	43–136	53.13 ± 1.76	136–255	41.07 ± 2.23
	O-15	0–37	2.04 ± 0.11	37–145	45.39 ± 2.21	145–255	54.36 ± 3.01
	Ref-30	0–57	14.54 ± 1.08	57–132	51.63 ± 2.70	132–255	35.83 ± 2.69
	S-30	0–41	6.03 ± 0.25	41–126	48.53 ± 2.35	126–255	42.48 ± 2.18
	O-30	0–42	9.74 ± 0.07	42–129	39.14 ± 1.68	129–255	55.16 ± 3.15

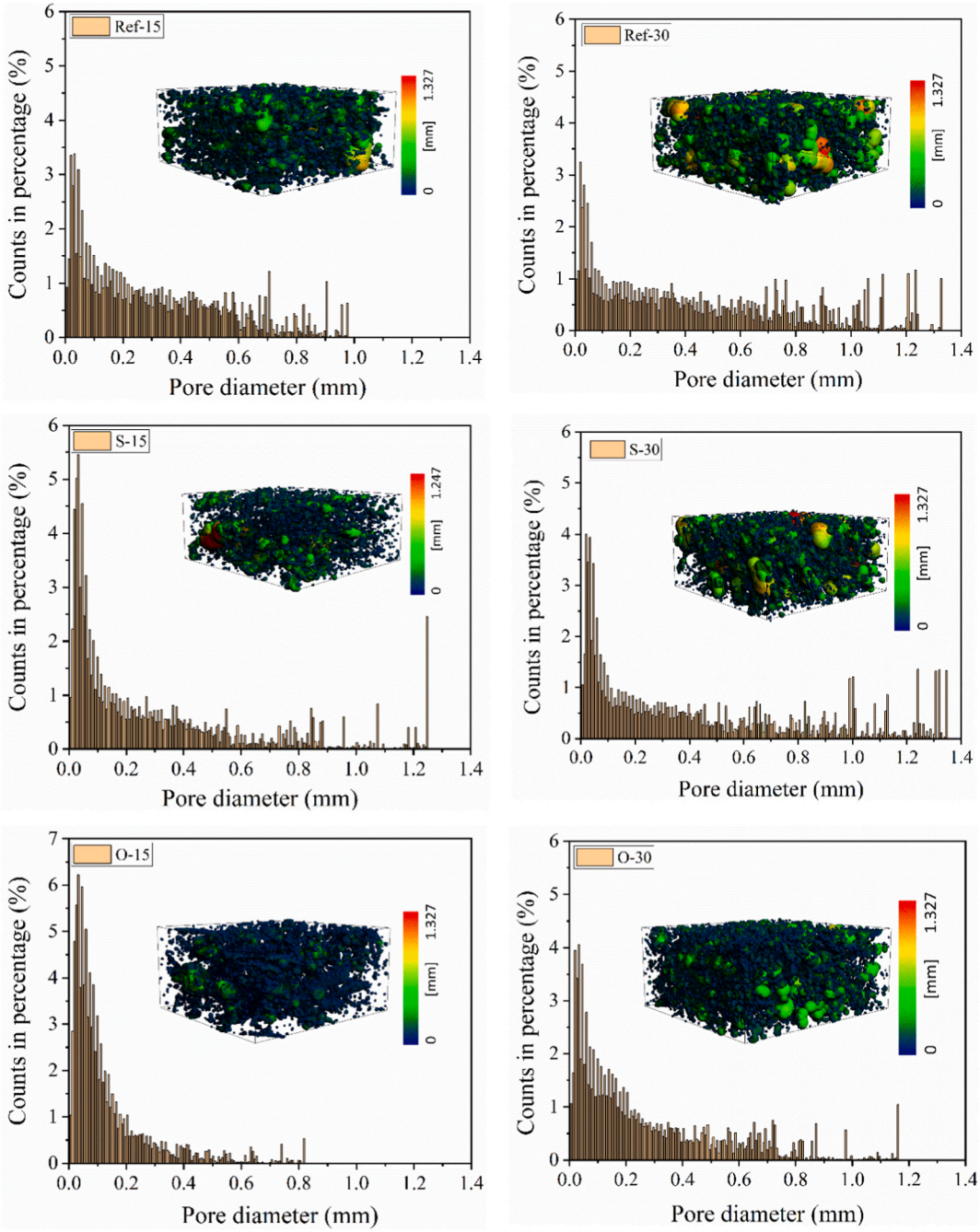

Fig. 7. The porosity of different BA-BCB samples by Micro CT.

observed from the 3D volumes that the percentage of the large pores in the blended binders with 30 % replacement is higher than that of 15 % replacement. The increment of BA mixing could release more hydrogen gas, leading to more and larger pores generated. In addition, it can be seen from the corresponding data that the pore count distribution in the BA-BCBs with natural fibers is more concentrated in the small-size range compared to those binders without natural fibers (Ref-15 and Ref-30). This indicates that natural fibers contribute to the reduction of larger pores through a filling effect. On the one hand, due to the existence of natural fibers, some small pores can be prevented from interconnecting to form large pores. On the other hand, the hollow lumen structure of natural fibers may act as channels for gas release, thereby reducing hydrogen gas accumulation and mitigating the formation of large pores in the BA-BCBs during the curing period. Therefore, natural fibers with larger diameters tend to provide a better pore-filling effect, as they are less likely to be obstructed by the pastes. For samples with OPF (Table 2), the pore diameter distribution is mostly focused on the smaller-size range compared to those samples with SF.

To summarize, for the micro-pore filling (below 2 mm), OPF incorporation has a more significant effect than SF incorporation, regardless of the BA addition level. For the naked-eye pores, the filling effect of OPF is less apparent as the increase of BA, while SF is still relatively evident due to fewer organic components (lignin and extractives). Thereby, it is recommended to incorporate SF into BA-BCBs, considering the stability of the filling effect at high BA utilization.

3.2. Microscopic performance

3.2.1. Hydration process

To study the influence of natural fiber additions on the hydration process of BA-BCBs, the BA-BCBs hydration heat release was determined by using an isothermal calorimeter. The results of hydration heat release are illustrated in Fig. 8.

The entire hydration process generally consists of four periods: dissolution period, induction period, acceleration/deceleration period, and stable period [51]. The first exothermic peak formation is due to rapid dissolution and the reaction of aluminates and sulfate from BA and the cement clinker initially within 1 h after mixing with water. Then the second exothermic peak comes with the hydration of C_3S and the formation of secondary C-S-H gel [52]. It can be seen from the enlarged picture in Fig. 8(a) that the samples with natural fibers have longer second-peak reached time and lower second-maximum heat release rates than their corresponding reference samples. This is mainly due to the incorporation of natural fibers, which leads to the retardation of the CEM-BA hydration. Especially for samples with oil palm fibers, the retardation is considerably prolonged by approximately 8 h for the O-15, and the second peaks for both O-15 and O-30 are the lowest in their groups (one group is a 15 % replacement level, and the other group is a 30 % replacement level), respectively. This is attributed to the high proportion of lignin and extractives in the oil palm fibers, which retard the cement hydration reaction by forming an organic layer coating around the anhydrous or partially hydrated cement grains [53]. In addition, with the increase of BA, the second exothermic peak of the binders with 30 % BA was greatly decreased, and the arrival time of their second peaks is delayed. This indicated that BA addition also results in a certain degree retarding of cement hydration. In fact, BA, due to lower reactivity, would dilute the clinker contents (alite and belite) when the equivalent cement was replaced [54]. Interestingly, it has to be mentioned that the time reaching the second exothermic peak for O-30 is shorter than that for O-15. This behavior is difficult to explain, and the most likely reason is that higher BA content generates more and larger pores, which are well-suited to the size of OPF. Consequently, OPF may facilitate a seeding effect, promoting heterogeneous nucleation and crystallization during the CEM–BA hydration process [55]. This effect could partially offset the hydration delay caused by the organic

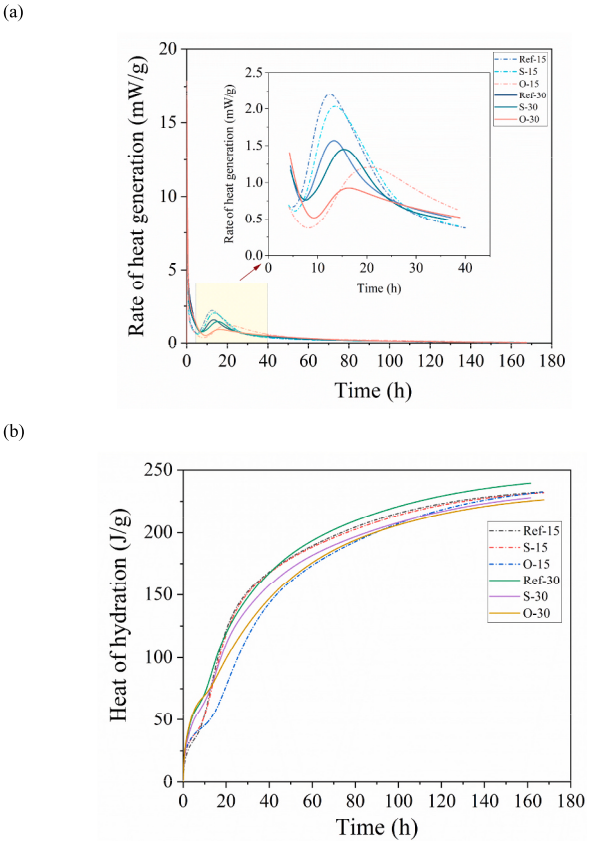

Fig. 8. Heat of hydration: (a) heat flow, (b) Total heat release.

components of OPF. As a result, the retarding effect in O-15 is more pronounced compared to O-30.

As can be seen from Fig. 8(b), Ref-30 has the highest total released heat, followed by Ref-15. This indicates that increasing the replacement level leads to greater cumulative heat generation. In other words, the addition of 15 % BA in the CEM-BA system contributes more cumulative heat than an equivalent amount of pure cement. This is primarily attributed to the additional sources of silica and alumina supplied by BA, which promote pozzolanic reaction and thus enhance heat evolution. This is confirmed by the result of the above XRF. On the other hand, both S-15 and O-15 are higher than both S-30 and O-30 regarding the total heat release. This suggests that when natural fibers are incorporated, the increasing replacement level with BA causes relatively poor pozzolanic reactivity in the BA-BCBs. The reason for this phenomenon is not yet clear until now, but this behavior is possibly related to the decrease in calcium source caused by both less cement amount and the capture of natural fibers on calcium.

3.2.2. XRD analysis

The XRD patterns compare the hydration products of the different samples at 3 and 28 days of curing (Fig. 9). Compared with the samples at 3 days, the portlandite peak is noticeably higher at 28 days in the mixtures containing natural fibers, whereas no significant change is observed in the binders without natural fibers. This indicates that the organic components of the natural fibers delay the hydration process, thereby reducing the consumption of CH during the secondary hydration stage [56]. This observation is consistent with the calorimetric analysis. Furthermore, a higher quartz peak intensity is observed as the BA replacement level rises, which can be attributed to the substantial quartz content in the BA. Notably, the broad peak associated with the Cl-LDH phase becomes more pronounced as the BA replacement level increases. This is likely due to the relatively higher alumina content and lower SO_4^{2-} content contained in the BA compared to the cement, which favours the formation of LDH phases. These products are known to effectively immobilize inorganic anions such as chlorides. The formation of Cl-LDH has not only been identified in the present study but has also been reported and confirmed in the literature [57,58].

3.2.3. TG-DTG analysis

The TG and DTG results of all tested samples for 28 d curing are shown in Fig. 10. Comparing the TG curves shown in Fig. 10(a) and (b), it can be seen that the mass loss of each binder sample is quite similar when the cement replacement ratio is 15 %, but when the replacement ratio is 30 % the degree of mass loss is obviously different. This indicates that when the BA addition is too large, the effect of natural fiber on the CEM-BA reaction is more evident.

The DTG curves could be generally divided into four stages. The first wide peaks at 40–200 C were attributed to the vaporization of unbound water (40–105 °C) and the decomposition of the hydration product C-S-H (105–200 °C); the second sharp peaks at 400–500 °C are the decomposition of portlandite ($Ca(OH)_2 \rightarrow CaO + H_2O$), and the peaks at 600–800 °C are related to calcite decarbonization $CaCO_3 \rightarrow CaO + CO_2$. Lastly, rare literature about the peak at 800–850 °C is reported. According to the metallic zinc that existed in BA, this peak is assumed to be associated with the volatilization of $ZnCl_2$ formed at temperatures above 800 °C [59,60]. Besides, it is noted that the small exothermic peaks located at around 280 °C are attributed to the thermal degradation of cellulose and lignin [61].

In comparison with the DTG curves, the peak of C-(A)-S-H for 30 % replacement level is higher than that for 15 % replacement level, while the peaks of both portlandite (CH) and calcite are reduced. This phenomenon also verifies the results of the XRD, which suggested that the portlandite produced by cement hydration was consumed due to the pozzolanic reaction of extra BA, thereby leading to a decrease in calcite and more amorphous C-(A)-S-H transformed.

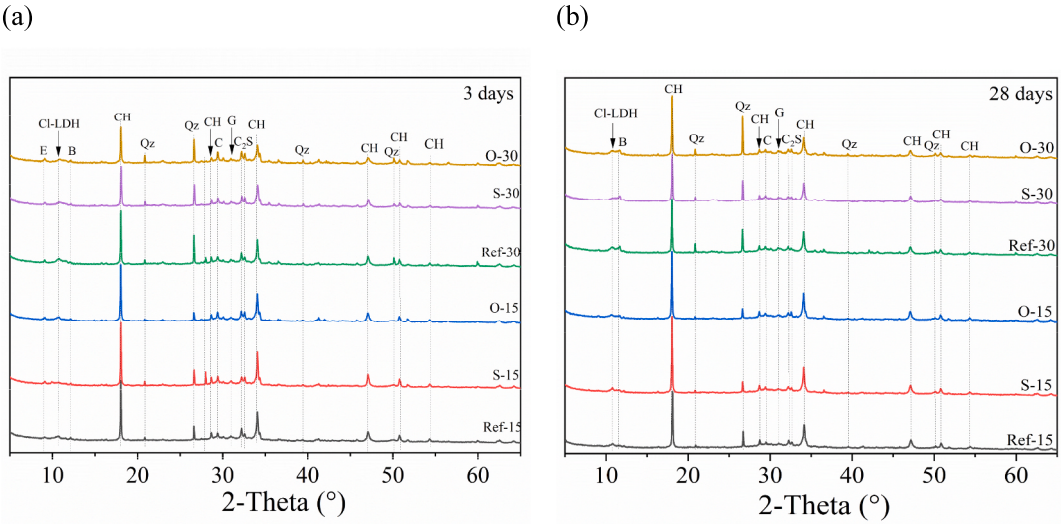

Fig. 9. XRD of all tested samples at 3 days and 28 days. Abbreviations associated with the mineralogical phase are: E-ettringite, Cl-LDH-chloride layered double hydroxide, B-brownmillite, G-gypsum, CH-portlandite, C-Calcite, Qz-quartz, C_2S-dicalcium silicate phase.

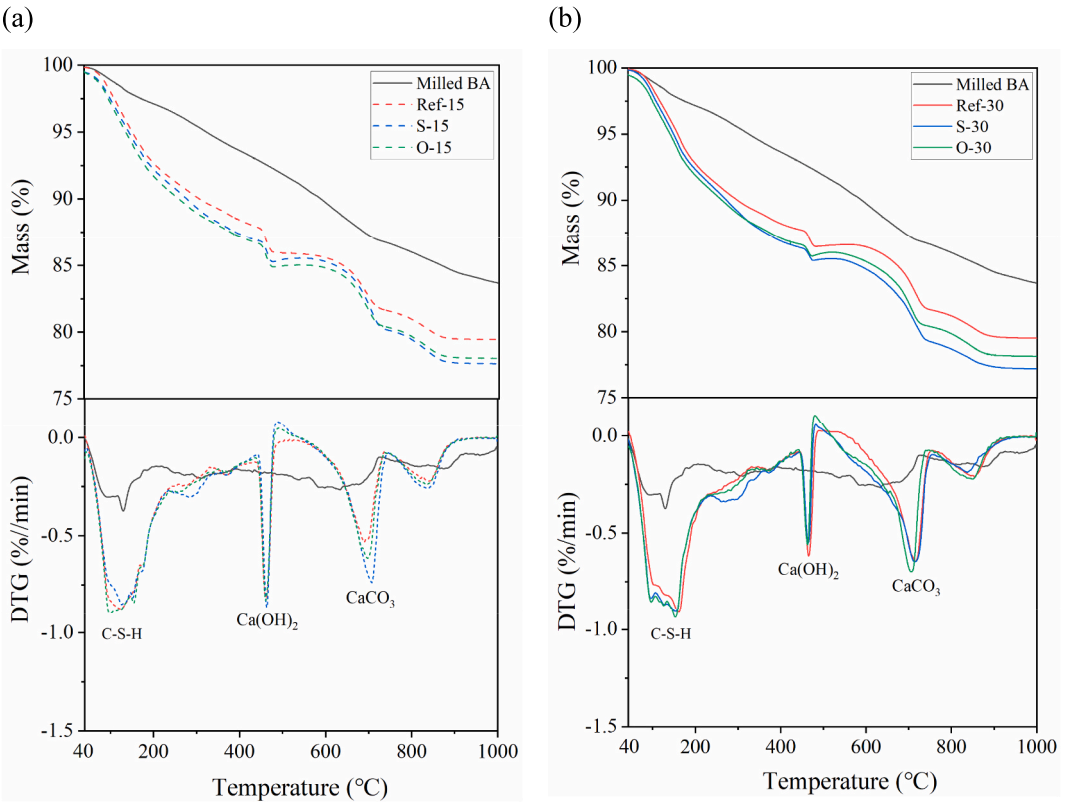

Fig. 10. TG-DTG results of all tested samples for 28 days.

3.2.4. *Contaminant leaching*

The leaching results of heavy metal ions and anions in all samples are summarized in Table 6. Even though the milled BA and unhydrated CEM I exhibited high levels of contaminant leaching, the concentrations of most ions in all BA-BCBs were significantly lower than the legislative limit, with the exception of Cu. This indicates that contaminant ions are immobilized by hydration products and fibre adsorption. The corresponding immobilization mechanisms are illustrated in Fig. 11. As shown, C–(A)–S–H gels can adsorb contaminant ions through SiO_4 tetrahedral substitution and Ca^{2+} cation exchange [62], thereby controlling their mobility. Meanwhile, the LDH phase can immobilize anionic species, such as chloride, via interlayer anion exchange, which is supported by the XRD results. Furthermore, when incorporating natural fibers into BA-BCBs, the leaching concentrations of contaminants have been significantly reduced. This effect can be attributed to fiber-assisted immobilization [63,64]. Natural fibers enhance immobilization through capillary suction facilitated by their hollow lumen structure [65]. Upon entering the inner structure, contaminant ions can be further stabilized by electrostatic attraction and binding by numerous hydroxyl groups [32,66]. Collectively, these mechanisms contribute to effective contaminant immobilization within the BA-BCB system, thereby reducing leaching.

It is worth mentioning that the slight exceedance of the Cu leaching limit may be attributed to two factors. First, the concentration of Cu in the milled BA is relatively higher than that of other heavy metals (e.g., Ni, Mo, Pb). Second, the fine particle size of the crushed samples used for the leaching test may have contributed to enhanced Cu release. Yang et al. [68] reported that the smaller the particle size of the crushed BA-based cement composites, lead to higher Cu leaching. Nevertheless, the results still indicate that natural fiber incorporation contributes to the mitigation of Cu leaching. In this case, the BA-BCBs can be alternatively applied in specific engineering applications, such as subgrade layers, pavement structures beneath bridges, covered parking areas, or intermediate layers in multi-layer wall systems, where direct contact with water is limited. Under such conditions, Cu is unlikely to be readily leached due to its limited migration potential.

Noticeably, the leaching of anions (chloride and sulfate) is considerably decreased compared with that of metal cations when plant fibers are incorporated. That means the fiber incorporation can reduce the risks of steel corrosion caused by chloride and the expansion issue caused by excessive sulfate. Comparing SF to OPF, the OPF has a more obvious absorption capacity for the anions. This could be explained by the denser lumen structures efficiently exerting the fiber capillary force to absorb the chloride and sulfate anions. In comparison with the above absorption effect, natural fiber addition has less reduction in the leaching of several heavy metal ions, possibly related to their relatively low concentrations in the BA-BCBs. Nevertheless, the heavy metal ions were still effectively immobilized, and the leaching results of heavy metal ions absorbed by incorporated plant fibers can basically comply with the Dutch soil environmental legislation [39].

Table 6
Leaching of anions (sulfate and chloride) and heavy metal ions present in the leachates for milled BA, CEM I 52.5 R, and all binder samples after 28 d curing; the units for concentrations given as mg per kg of dry matter; LL is the legislation limit [39].

Samples	Leaching value /mg/kg d.m.							
	Chloride	Sulfate	Ni	Cu	Zn	Mo	Pb	pH
Milled BA	8682	13865	0.18	7.01	0.84	3.77	0.56	9.8
CEM I 52.5 R [67]	322	52	20.5	<0.01	0.05	0.2	17	–
Ref-15	291.4	38.4	0.23	1.52	0.21	0.1	0.69	13.68
S-15	252.3	28.5	0.09	1.02	0.17	0.09	0.58	13.64
O-15	242.8	27.7	0.15	1.1	0.18	0.1	0.58	13.6
Ref-30	533.3	36.9	0.12	1.84	0.38	0.13	0.89	13.51
S-30	477.9	31.6	0.1	1.3	0.33	0.11	0.72	13.25
O-30	455.1	21.7	0.11	1.31	0.36	0.12	0.75	13.18
LL	616	1730	0.44	0.9	4.5	1	2.3	–

- Not measured.

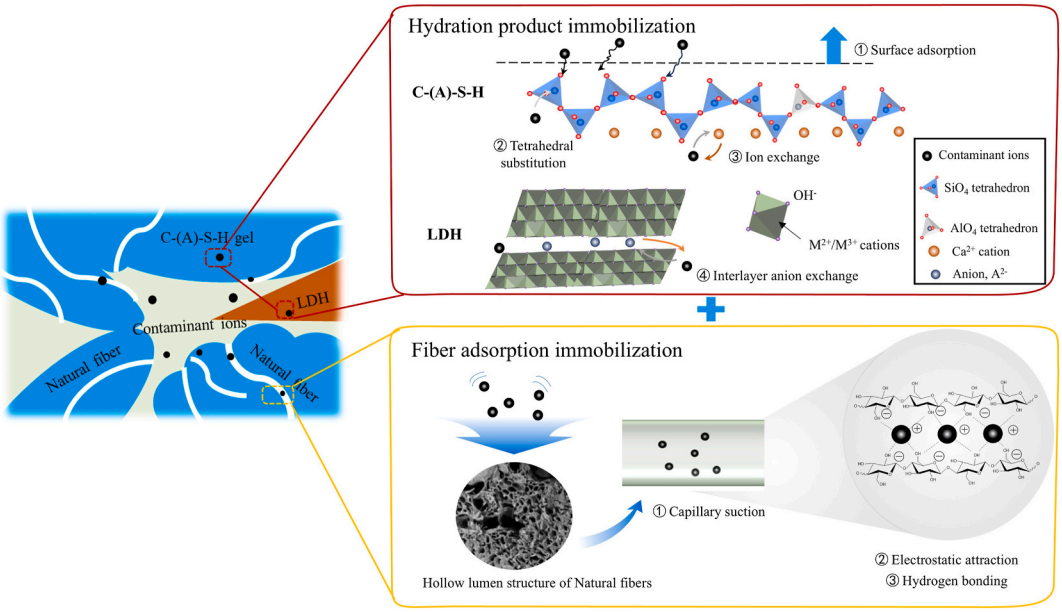

Fig. 11. Immobilization mechanism of contaminant ions in the BA-BCBs system.

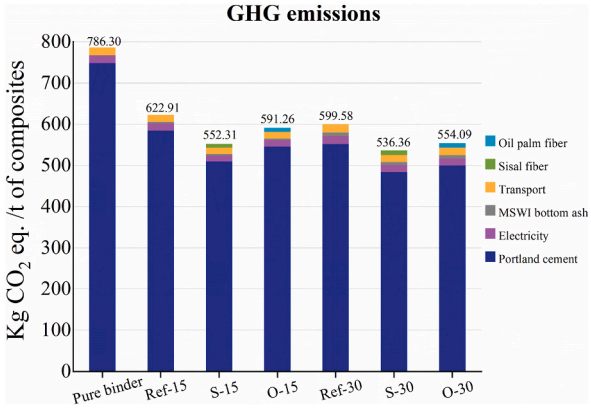

Fig. 12. GHG emissions of all tested samples.

3.3. Environmental and economic assessment

3.3.1. Greenhouse gas (GHG) emissions

GHG emissions for one ton of binder composites are shown in Fig. 12. The data show that the BA-based binders with or without natural fibers have lower GHG emissions than pure cement binders. This is because the waste BA or natural fibers incorporation reduces the dosage of cement in the binder, hence decreasing the GHG emission from the production of cement. Additionally, it has to be mentioned that the incorporation of natural fibers mixed into binders can reduce GHG emissions when the cement replacement keeps the same level. Especially, SF reinforcement has a better decrease in GHG emissions than OPF. For samples with 30 % replacement, the GHG emissions of S-30 are reduced by around 63 kg CO_2 eq./ton compared to the Ref-30, exceeding the relative reduction of O-30 emissions (45 kg CO_2 eq./ton). This indicates that S-30 has an advantage in carbon dioxide emissions compared to other samples, which have great potential for building applications.

3.3.2. Economic evaluation

To evaluate the cost-benefit of the BA-based binders containing SF and OF, a cost-benefit analysis is carried out for pure cement binders and six different binder samples. The price of raw materials for binders comes from the local market price in the Netherlands, shown in Table 7. It is noted that the cost of BA and its relevant transport is free. One reason is that BA is a waste material. Another, for the municipal waste incineration plant, the fee for BA landfilling or other treatments is far higher than that of transport for the BA-based binders' preparation. Fig. 13 shows a cost-benefit analysis of all binder samples. As shown, the cost of the BA-based binders remarkably reduced with the increase in the replacement level of BA. In addition, it can be seen that even though natural fibers were incorporated into the relevant BA-based binders, the cost gap between them was almost negligible. This is because natural fibers chosen in our current work are a bulk commodity and very cheap (Table 7). In the future, if this technique is further optimized and validated, waste natural fibers could be utilized. This would not only generate huge economic benefits but also contribute to reducing the environmental burden associated with fiber waste. Thus, S-30 can be considered to be a suitable mix design considering its compressive strength, leaching, economic benefit, and waste utilization rate.

4. Conclusions

Two types of natural fibers (SF and OPF) were incorporated and evaluated to investigate their effects on the mechanical properties and leaching behavior of the BA-BCBs. And the different replacement of BA was studied. Moreover, the environmental and economic feasibility of the natural fiber-reinforced binders was evaluated. Based on the findings of this study, the following conclusions can be drawn.

(1) In the BA-based cement binders, natural fiber incorporation has a positive impact on the compressive strength of the BA-BCBs, due to the filling effect. Especially, the compressive strength of SF incorporation increases by 85 % compared to the reference sample at 28-day curing when the replacement level is 30 wt%. Further, it is found that S-30 has acceptable compressive strength, which meets some types of road pavement requirements under the premise of BA maximum consumption.
(2) The increase of cement replacement with BA leads to larger and more pores generated in the BA-BCBs, which is attributed to more hydrogen gas release, while natural fibers incorporation considerably reduces the size and numbers of the pores on account of the obstacle of natural fiber on gas diffusion and pore interconnection. Furthermore, the micro-CT study has proved that natural fiber with a larger diameter is more beneficial for pore filling in the BA-BCBs.
(3) Although the filling effect of natural fibers effectively enhances the strength of BA-BCBs, the fiber addition also delays the early cement hydration due to some organic components (extractives and lignin) as cement retarders; consequently, it negatively affects the strength of BA-BCBs development. Eventually, OPF, with a higher proportion of these organic components, apparently reduces the contribution to compressive strength by the filling effect.
(4) The incorporation of natural fibers reduces the leaching of chlorides, sulfates, and heavy metal ions due to their capillary suction effect. This reduction is particularly pronounced for anions, while the effect on heavy metal ion leaching is comparatively less significant.
(5) The GHG emission results obtained from the LCA analysis indicate that the incorporation of waste BA and natural fibers significantly reduces greenhouse gas emissions by increasing the cement replacement level, thereby mitigating the environmental impact.

Table 7
Prices of raw materials and processing for all tested samples.

	Raw materials					Process	
	OPC	MSWI BA	Water	Natural fibers		Electricity	Transport
				SF	OPF		
$Price_{(approx.)}$	123 €/ton	–	0.87 €/m^3	10 €/ton	15 €/ton	0.32 €/kWh	0.348 €/tkm

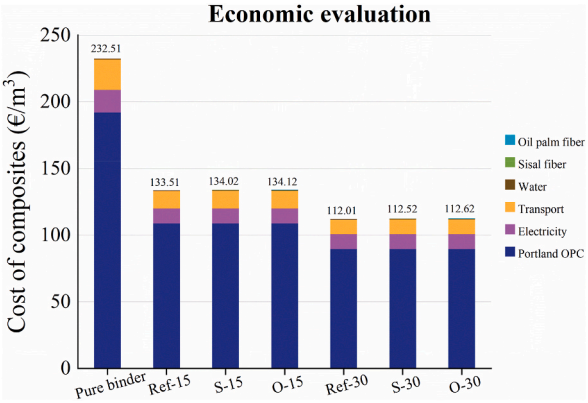

Fig. 13. Cost of one cubic meter of BA-BCB samples (€/m^3).

(6) In terms of economic feasibility, replacing cement with BA substantially reduced the overall cost of the BA-BCBs by approximately 52 %, while the incorporation of natural fibers resulted in only a negligible cost increase. Furthermore, if waste natural fibers are utilized, the cost efficiency of BA-BCB production could be further enhanced, making this technique even more economically attractive.

To conclude, both SF and OPF demonstrate significant potential as sustainable reinforcements, contributing to improved mechanical performance, contaminant immobilization capacity, and overall environmental sustainability. Among the investigated formulations, the incorporation of SF is particularly recommended for BA-BCBs, especially at a 30 % cement replacement with BA. This combination effectively enhances mechanical strength, promotes microstructural densification, and improves the immobilization of hazardous ions, while simultaneously reducing carbon emissions and exerting minimal adverse effects on economic cost. Based on these considerations, the S-30 mixture exhibits the highest potential for practical engineering applications. Further investigations are warranted to optimize the mixture design and assess the feasibility of other waste-derived fibers as reinforcement materials in cementitious composites containing BA.

CRediT authorship contribution statement

Helong Song: Writing – original draft, Methodology, Investigation, Formal analysis, Data curation, Conceptualization, Funding acquisition. **Florent Gauvin:** Writing – review & editing, Supervision. **Tao Liu:** Writing – review & editing, Methodology, Investigation, Conceptualization. **Xiaohui Sun:** Writing – review & editing. **Zijun Dong:** Writing – review & editing. **Feng Wang:** Writing – review & editing. **Xiangsheng Chen:** Writing – review & editing. **H.J.H. Brouwers:** Writing – review & editing, Supervision.

Declaration of competing interest

The authors declare that they have no known competing financial interests or personal relationships that could have appeared to influence the work reported in this paper.

Acknowledge

This research is supported by the National Natural Science Foundation of China (Grant No. 52500171), the National Natural Science Foundation of China Excellent Young Scientists Fund (Grant No. 52422004), and the Third Phase of High-Level University Construction (No.000001033378), the College of Civil and Transportation Engineering of Shenzhen University (China), Key Laboratory of Coastal Urban Soil-Water Environmental Evolution, Ministry of Ecology and Environment (under construction) of Shenzhen University (China) and the Department of the Built Environment of Eindhoven University of Technology (the Netherlands). The authors thank Zixing Liu for help on the TG test, Yan Luo for help on the Micro-CT test, Dipl. Min. K. Schollbach for help on the supply of MSWI bottom ash, and Dr. J. E.G. van Dam (Wageningen University, the Netherlands) for the supply of natural fibers.

Data availability

Data will be made available on request.

References

[1] A. Maalouf, A. Mavropoulos, Re-assessing global municipal solid waste generation, Waste Manag. Res. 41 (4) (2022) 936, https://doi.org/10.1177/0734242X221074116.

[2] A.P. Clasen, F. Agostinho, C.M. Almeida, G. Liu, B.F. Giannetti, Advancing towards circular economy: environmental benefits of an innovative biorefinery for municipal solid waste management, Sustain. Prod. Consum. 46 (2024) 571–581, https://doi.org/10.1016/j.spc.2024.03.015.

[3] P.Z. Oo, T. Prapaspongsa, V. Strezov, N. Huda, K. Oshita, M. Takaoka, J. Ren, A. Halog, S.H. Gheewala, The role of global waste management and circular economy towards carbon neutrality, Sustain. Prod. Consum. 52 (2024) 498–510, https://doi.org/10.1016/j.spc.2024.11.021.

[4] J. Hu, R. Niu, J. Liu, W. Zhang, J. Liu, F. Xing, The hydration and heavy metal immobilization performance of the CO2-active incineration fly ash-calcined clay-cement (CFC3) composite low-carbon cementitious system, Cem. Concr. Compos. 149 (2024) 105528, https://doi.org/10.1016/j.cemconcomp.2024.105528.

[5] B. Chen, P. Perumal, C. Liu, Y. Chen, C. Chang, M. Pavlin, D. Kvočka, V. Ducman, T. Luukkonen, M. Illikainen, Municipal solid waste incineration (MSWI) bottom ash-blended cementitious materials: performance, challenges, and potential solutions, Crit. Rev. Environ. Sci. Technol. 55 (19) (2025) 1506–1533, https://doi.org/10.1080/10643389.2025.2548287.

[6] Y. Cheng, G. Gao, L. Chen, W. Du, W. Mu, Y. Yan, H. Sun, Physical and mechanical study of municipal solid waste incineration (MSWI) bottom ash with different particle size distribution, Constr. Build. Mater. 416 (2024) 135137, https://doi.org/10.1016/j.conbuildmat.2024.135137.

[7] B. Chen, G. Ye, The role of water-treated municipal solid waste incineration (MSWI) bottom ash in microstructure formation and strength development of blended cement pastes, Cement Concr. Res. 178 (2024) 107440, https://doi.org/10.1016/j.cemconres.2024.107440.

[8] N. De Belie, A.M. Joseph, S. Matthys, Reactivity of Municipal Solid Waste Incineration Ashes as a Supplementary Cementitious Material, 15th International Congress on the Chemistry of Cement (ICCC19), ICCC, Prague, Czech Republic, 2019.

[9] B. Chen, J. Chen, F.F. de Mendonça Filho, Y. Sun, M.B. van Zijl, O. Copuroglu, G. Ye, Characterization and mechanical removal of metallic aluminum (Al) embedded in weathered municipal solid waste incineration (MSWI) bottom ash for application as supplementary cementitious material, Waste Manage. (Tucson, Ariz.) 176 (2024) 128–139, https://doi.org/10.1016/j.wasman.2024.01.031.

[10] L. Biganzoli, L. Gorla, S. Nessi, M. Grosso, Volatilisation and oxidation of aluminium scraps fed into incineration furnaces, Waste Manage. (Tucson, Ariz.) 32 (12) (2012) 2266–2272, https://doi.org/10.1016/j.wasman.2012.06.003.

[11] N.M. Alderete, A.M. Joseph, P. Van den Heede, S. Matthys, N. De Belie, Effective and sustainable use of municipal solid waste incineration bottom ash in concrete regarding strength and durability, Resour. Conserv. Recycl. 167 (2021) 105356, https://doi.org/10.1016/j.resconrec.2020.105356.

[12] Y. Liu, K.S. Sidhu, Z. Chen, E.-H. Yang, Alkali-treated incineration bottom ash as supplementary cementitious materials, Constr. Build. Mater. 179 (2018) 371–378, https://doi.org/10.1016/j.conbuildmat.2018.05.231.

[13] N. Saikia, G. Mertens, K. Van Balen, J. Elsen, T. Van Gerven, C. Vandecasteele, Pre-treatment of municipal solid waste incineration (MSWI) bottom ash for utilisation in cement mortar, Constr. Build. Mater. 96 (2015) 76–85, https://doi.org/10.1016/j.conbuildmat.2015.07.185.

[14] A.M. Joseph, R. Snellings, P. Nielsen, S. Matthys, N. De Belie, Pre-treatment and utilisation of municipal solid waste incineration bottom ashes towards a circular economy, Constr. Build. Mater. 260 (2020) 120485, https://doi.org/10.1016/j.conbuildmat.2020.120485.

[15] P. Tang, M.V.A. Florea, P. Spiesz, H.J.H. Brouwers, Characteristics and application potential of municipal solid waste incineration (MSWI) bottom ashes from two waste-to-energy plants, Constr. Build. Mater. 83 (2015) 77–94, https://doi.org/10.1016/j.conbuildmat.2015.02.033.

[16] Y. Huang, L. Wang, T. Wu, W. Liu, Q. Tang, Mechanical properties and heavy metal leaching behaviors of municipal solid waste incineration bottom ash as road embankment fillings, J. Clean. Prod. 394 (2023) 136355, https://doi.org/10.1016/j.jclepro.2023.136355.

[17] Q. Alam, K. Schollbach, M.V.A. Florea, H.J.H. Brouwers, Investigating washing treatment to minimize leaching of chlorides and heavy metals from MSWI bottom ash. 4th International Conference on Sustainable Solid Waste Management, Limasol, Cyprus, 2016.

[18] P. Ingold, G. Weibel, P. Kämpfer, S.V. Churakov, Weathering and trace element mobilisation of MSWI bottom ash from wet and dry extraction, J. Contam. Hydrol. 272 (2025) 104566, https://doi.org/10.1016/j.jconhyd.2025.104566.

[19] X. Sun, Y. Yi, Acid washing of incineration bottom ash of municipal solid waste: effects of pH on removal and leaching of heavy metals, Waste Manage. (Tucson, Ariz.) 120 (2021) 183–192, https://doi.org/10.1016/j.wasman.2020.11.030.

[20] Z. Chen, J.-S. Li, D. Xuan, C.S. Poon, X. Huang, Effect of alkaline washing treatment on leaching behavior of municipal solid waste incineration bottom ash, Environ. Sci. Pollut. Control Ser. 30 (1) (2023) 1966–1978, https://doi.org/10.1007/s11356-022-22073-1.

[21] S. Pal, M. Shariq, H. Abbas, A. Pandit, A. Masood, Strength characteristics and microstructure of hooked-end steel fiber reinforced concrete containing fly ash, bottom ash and their combination, Constr. Build. Mater. 247 (2020) 118530, https://doi.org/10.1016/j.conbuildmat.2020.118530.

[22] M. Hanafi, E. Aydin, A. Ekinci, Engineering properties of basalt fiber-reinforced bottom ash cement paste composites, Materials 13 (8) (2020) 1952, https://doi.org/10.3390/ma13081952.

[23] Y. Cheng, X. Huang, Application of municipal solid waste incineration bottom ash into engineered cementitious composites, Int. J. Pavement Res. Technol. 15 (5) (2022) 1106–1117, https://doi.org/10.1007/s42947-021-00075-5.

[24] D. Singh, A. Kumar, Performance studies of fiber-reinforced municipal solid waste incineration bottom ash amended with cement for geotechnical applications, Sādhanā 48 (3) (2023) 117, https://doi.org/10.1007/s12046-023-02171-7.

[25] L. Li, T. Zang, H. Xiao, W. Feng, Y. Liu, Experimental study of polypropylene fibre-reinforced clay soil mixed with municipal solid waste incineration bottom ash, Eur. J. Environ. Civil Eng. 27 (8) (2023) 2700–2716, https://doi.org/10.1080/19648189.2020.1795726.

[26] S. Pochalard, C. Wungsumpow, K. Piriyakul, Enhancement of compressive strength in cement admixed Bangkok clay with glass fiber and bottom ash for eco-friendly functional road materials, Macromol. Mater. Eng. 12 (2025) 279–292, https://doi.org/10.22075/macs.2024.33848.1653.

[27] F.Z. Youssari, O. Taleb, A.S. Benosman, Towards understanding the behavior of fiber-reinforced concrete in aggressive environments: acid attacks and leaching, Constr. Build. Mater. 368 (2023) 130444.

[28] W. Zhang, D. Shi, Z. Shen, W. Shao, L. Gan, Y. Yuan, P. Tang, S. Zhao, Y. Chen, Reduction of the calcium leaching effect on the physical and mechanical properties of concrete by adding chopped basalt fibers, Constr. Build. Mater. 365 (2023) 130080.

[29] F.M. Khan, A.H. Shah, S. Wang, S. Mehmood, J. Wang, W. Liu, X. Xu, A comprehensive review on epoxy biocomposites based on natural fibers and bio-fillers: challenges, recent developments and applications, Adv. Fiber Mater. 4 (4) (2022) 683–704, https://doi.org/10.1007/s42765-022-00143-w.

[30] Y. Zheng, J. Wang, Y. Zhu, A. Wang, Research and application of kapok fiber as an absorbing material: a mini review, J. Environ. Sci. 27 (2015) 21–32, https://doi.org/10.1016/j.jes.2014.09.026.

[31] N.A. Zubair, R.M. Moawia, M.M. Nasef, M. Hubbe, M. Zakeri, A critical review on natural fibers modifications by graft copolymerization for wastewater treatment, J. Polym. Environ. 30 (4) (2022) 1199–1227, https://doi.org/10.1007/s10924-021-02269-1.

[32] A. Kausar, S.T. Zohra, S. Ijaz, M. Iqbal, J. Iqbal, I. Bibi, S. Nouren, N. El Messaoudi, A. Nazir, Cellulose-based materials and their adsorptive removal efficiency for dyes: a review, Int. J. Biol. Macromol. (2022), https://doi.org/10.1016/j.ijbiomac.2022.10.220.

[33] B.A. Akinyemi, C. Dai, Development of banana fibers and wood bottom ash modified cement mortars, Constr. Build. Mater. 241 (2020) 118041, https://doi.org/10.1016/j.conbuildmat.2020.118041.

[34] Food and Agriculture Organ Unit. Nation. Jute, kenaf, sisal, abaca, coir and allied fibres statistical bulletin 2023. 2024. https://www.fao.org/markets-and-trade/commodities-overview/fibres/jute-and-hard-fibres/en. (Accessed 23 January 2026).

[35] A. Mohanty, M.a. Misra, G. Hinrichsen, Biofibres, biodegradable polymers and biocomposites: an overview, Macromol. Mater. Eng. 276 (1) (2000) 1–24, https://doi.org/10.1002/(SICI)1439-2054(20000301)276:1.

[36] S. Shinoj, R. Visvanathan, S. Panigrahi, M. Kochubabu, Oil palm fiber (OPF) and its composites: a review, Ind. Crop. Prod. 33 (1) (2011) 7–22, https://doi.org/10.1016/j.indcrop.2010.09.009.

[37] A.C. dos Santos, F.G. Cardoso, R.J. da Silva, H. de Fátima Gorgulho, T.H. Panzera, Modification of short sugarcane bagasse fibres for application in cementitious composites: a statistical approach to mechanical and physical properties, Constr. Build. Mater. 353 (2022) 129072.

[38] Y. Luo, K. Klima, H.J.H. Brouwers, Q. Yu, Effects of ladle slag on Class F fly ash geopolymer: reaction mechanism and high temperature behavior, Cem. Concr. Compos. 129 (2022) 104468, https://doi.org/10.1016/j.cemconcomp.2022.104468.

[39] S.Q. Decree, Regulation of the state secretary for housing, planning and the environment and the state secretary for transport: preliminary draft of the soil quality regulation. https://rwsenvironment.eu/subjects/soil/legislation-and/soil-quality-decree/, 2007. (Accessed 12 February 2023).

[40] M.U. Hossain, C.S. Poon, I.M. Lo, J.C. Cheng, Comparative LCA on using waste materials in the cement industry: a Hong Kong case study, Resour. Conserv. Recycl. 120 (2017) 199–208, https://doi.org/10.1016/j.resconrec.2016.12.012.
[41] Y. Rhaouti, Y. Taha, M. Benzaazoua, Assessment of the environmental performance of blended cements from a life cycle perspective: a systematic review, Sustain. Prod. Consum. 36 (2023) 32–48, https://doi.org/10.1016/j.spc.2022.12.010.
[42] International Organization for Standardization, Environmental Management, Life cycle assessment. Requirements and guidelines, ISO 14044:2006 (2006).
[43] S. Alnezami, G. Lamaa, M.F.C. Pereira, R. Kurda, J. de Brito, R.V. Silva, A sustainable treatment method to use municipal solid waste incinerator bottom ash as cement replacement, Constr. Build. Mater. 423 (2024) 135855, https://doi.org/10.1016/j.conbuildmat.2024.135855.
[44] Y. Song, B. Li, E.-H. Yang, Y. Liu, T. Ding, Feasibility study on utilization of municipal solid waste incineration bottom ash as aerating agent for the production of autoclaved aerated concrete, Cem. Concr. Compos. 56 (2015) 51–58, https://doi.org/10.1016/j.cemconcomp.2014.11.006.
[45] O. Gencel, S.M.S. Kazmi, M.J. Munir, G. Kaplan, O.Y. Bayraktar, D.O. Yarar, A. Karimipour, M.R. Ahmad, Influence of bottom ash and polypropylene fibers on the physico-mechanical, durability and thermal performance of foam concrete: an experimental investigation, Constr. Build. Mater. 306 (2021) 124887, https://doi.org/10.1016/j.conbuildmat.2021.124887.
[46] J. Girones, L.T. Vo, G. Mouille, J.O. Narciso, S. Arnoult, M. Brancourt-Hulmel, P. Navard, C. Lapierre, Impact of miscanthus lignin and arabinoxylan on Portland cement, Ind. Crop. Prod. 188 (2022) 115585, https://doi.org/10.1016/j.indcrop.2022.115585.
[47] M. Rachmat, T. Salsabilla, Analysis of hexagonal paving block as a better paving shape, IOP Conf. Ser. Mater. Sci. Eng., IOP Publishing Ltd (2019) 12068.
[48] Z. Chen, E.-H. Yang, Early age hydration of blended cement with different size fractions of municipal solid waste incineration bottom ash, Constr. Build. Mater. 156 (2017) 880–890, https://doi.org/10.1016/j.conbuildmat.2017.09.063.
[49] S. Ajouguim, J. Page, C. Djelal, M. Waqif, L. Saâdi, Impact of Alfa fibers morphology on hydration kinetics and mechanical properties of cement mortars, Constr. Build. Mater. 293 (2021) 123514, https://doi.org/10.1016/j.conbuildmat.2021.123514.
[50] G. Fang, M. Zhang, The evolution of interfacial transition zone in alkali-activated fly ash-slag concrete, Cement Concr. Res. 129 (2020) 105963, https://doi.org/10.1016/j.cemconres.2019.105963.
[51] X. Gao, Q. Yu, H.J.H. Brouwers, Reaction kinetics, gel character and strength of ambient temperature cured alkali activated slag–fly ash blends, Constr. Build. Mater. 80 (2015) 105–115, https://doi.org/10.1016/j.conbuildmat.2015.01.065.
[52] S. Liu, L. Wang, Y. Gao, B. Yu, W. Tang, Influence of fineness on hydration kinetics of supersulfated cement, Thermochim. Acta 605 (2015) 37–42, https://doi.org/10.1016/j.tca.2015.02.013.
[53] X. Zhang, L. Pel, D. Smeulders, Influence of water-soluble leachates from natural fibers on the hydration and microstructure of cement paste studied by nuclear magnetic resonance, Cement Concr. Res. 185 (2024) 107629, https://doi.org/10.1016/j.cemconres.2024.107629.
[54] V. Caprai, F. Gauvin, K. Schollbach, H.J.H. Brouwers, MSWI bottom ash as binder replacement in wood cement composites, Constr. Build. Mater. 196 (2019) 672–680, https://doi.org/10.1016/j.conbuildmat.2018.11.153.
[55] H. Song, T. Liu, F. Gauvin, H. Brouwers, Investigation of sisal fiber incorporation on engineering properties and sustainability of lightweight aggregates produced from municipal solid waste incinerated bottom ash, Constr. Build. Mater. 413 (2024) 134943, https://doi.org/10.1016/j.conbuildmat.2024.134943.
[56] Q. Wang, S. Li, S. Pan, X. Cui, D.J. Corr, S.P. Shah, Effect of graphene oxide on the hydration and microstructure of fly ash-cement system, Constr. Build. Mater. 198 (2019) 106–119, https://doi.org/10.1016/j.conbuildmat.2018.11.199.
[57] P. Tang, M.V.A. Florea, P. Spiesz, H.J.H. Brouwers, Application of thermally activated municipal solid waste incineration (MSWI) bottom ash fines as binder substitute, Cem. Concr. Compos. 70 (2016) 194–205, https://doi.org/10.1016/j.cemconcomp.2016.03.015.
[58] V. Caprai, K. Schollbach, M.V.A. Florea, H.J.H. Brouwers, Evaluation of municipal solid waste incineration filter cake as supplementary cementitious material, Constr. Build. Mater. 250 (2020) 118833, https://doi.org/10.1016/j.conbuildmat.2020.118833.
[59] J. Yao, Q. Kong, H. Zhu, Y. Long, D. Shen, Content and fractionation of Cu, Zn and Cd in size fractionated municipal solid waste incineration bottom ash, Ecotoxicol. Environ. Saf. 94 (2013) 131–137, https://doi.org/10.1016/j.ecoenv.2013.05.014.
[60] M. Díaz-Bautista, R. Álvarez-Rodríguez, C. Clemente-Jul, A. Mastral, AFBC of coal with tyre rubber. Influence of the co-combustion variables on the mineral matter of solid by-products and on Zn lixiviation, Fuel 106 (2013) 10–20, https://doi.org/10.1016/j.fuel.2012.12.041.
[61] S. Kumar, L. Prasad, P.P. Bijlwan, A. Yadav, Thermogravimetric analysis of lignocellulosic leaf-based fiber-reinforced thermosets polymer composites: an overview, Biomass Convers. Biorefinery 14 (12) (2024) 12673–12698, https://doi.org/10.1007/s13399-022-03332-0.
[62] G. Qiao, D. Hou, W. Li, B. Yin, Y. Zhang, P. Wang, Molecular insights into migration of heavy metal ion in calcium silicate hydrate (CSH) surface and intra-CSH (Ca/Si= 1.3), Constr. Build. Mater. 365 (2023) 130097, https://doi.org/10.1016/j.conbuildmat.2022.130097.
[63] C.M. Futalan, A.E.S. Choi, H.G.O. Soriano, M.K.B. Cabacungan, J.C. Millare, Modification strategies of kapok fiber composites and its application in the adsorption of heavy metal ions and dyes from aqueous solutions: a systematic review, Int. J. Environ. Res. Publ. Health 19 (5) (2022) 2703.
[64] N.S.A. Rahman, M.F. Yhaya, B. Azahari, W.R. Ismail, Utilisation of natural cellulose fibres in wastewater treatment, Cellulose 25 (2018) 4887–4903.
[65] R. De Gutiérrez, L. Diaz, S. Delvasto, Effect of pozzolans on the performance of fiber-reinforced mortars, Cem. Concr. Compos. 27 (5) (2005) 593–598.
[66] J. Kaur, P. Sengupta, S. Mukhopadhyay, Critical review of bioadsorption on modified cellulose and removal of divalent heavy metals (Cd, Pb, and Cu), Ind. Eng. Chem. Res. 61 (5) (2022) 1921–1954.
[67] E. Loginova, K. Schollbach, M. Proskurnin, H.J.H. Brouwers, Municipal solid waste incineration bottom ash fines: transformation into a minor additional constituent for cements, Resour. Conserv. Recycl. 166 (2021) 105354, https://doi.org/10.1016/j.resconrec.2020.105354.
[68] Z. Yang, S. Tian, L. Liu, X. Wang, Z. Zhang, Recycling ground MSWI bottom ash in cement composites: long-term environmental impacts, Waste Manage. (Tucson, Ariz.) 78 (2018) 841–848, https://doi.org/10.1016/j.wasman.2018.07.002.